Design and Operation of a Methane Absorption Stabilized Laser Strainmeter

J. Levine*

Joint Institute for Laboratory Astrophysics
National Bureau of Standards and University of Colorado
Boulder, Colorado 80302

ABSTRACT

A unique 30-meter laser strainmeter is described. The sytem uses a Fabry-Perot geometry and dynamically adjusts the frequency of the illuminating laser to follow a single fringe. The reference length for the system is provided by a second laser whose wavelength is stabilized using a vibration-rotation absorption line in methane. The system shows excellent sensitivity, wide bandwidth and essentially no drift. The instrument is being used to study several problems of geophysical and astrophysical interest including the earth tides and the free oscillations of the earth and in a search for gravitational waves.

*Staff Member, Quantum Electronics Division, National Bureau of Standards.

INTRODUCTION

In this paper we describe the construction of a novel and very sensitive 30-meter laser strainmeter. The system is unique in that it effectively uses a molecular transition as the length standard. It is therefore free from many of the drift problems that plague conventional quartz-rod strainmeters, while at the same time offering a number of distinct advantages such as wide bandwidth, absolute calibration and digital output.

We expect that the geophysical significance of this new type of instrumentation will generally be apparent to the reader. However, as interferometric devices are only recently coming into wide use in geophysical instrumentation, we present a rather complete description of the electro-optical system and the criteria used in its design. Discussions of the optical frequency length standard is presented after a description of the basic interferometer.

We are currently using the interferometer in several different experiments of geophysical interest.

The first is a long term measurement of the earth tides. Conventional quartz-rod strainmeters produce tidal records which are often contaminated by diurnal thermal cycling and/or instrumental drift. Our instrument should produce good quality tidal records which will make possible a meaningful comparison between the theory of strain tides and the observations. As a bonus these observations will yield information about secular strain rates and strain steps following seismic events.

The second experiment of geophysical interest is a measurement of the power spectrum of the earth's vibrations. We are especially interested in this power spectrum immediately following nuclear explosions and earthquakes. An analysis of the high frequency components ($\gtrsim$ 1 Hz) may prove to be useful as a discriminant, while the low frequency components ($\sim$ 1 cycle per hour)

give information on the earth's normal modes. Signal estimates suggest that these normal mode excitations might be detectable following a large (magnitude 7.5-8) earthquake.

DESCRIPTION OF THE APPARATUS

Long-Path Interferometer. The instrument is located in the Poorman's Relief Mine, an unworked gold mine approximately 5 miles west of Boulder, Colorado. The mine's approximate coordinates are 40° 1' N and 105° 20' W. The geology of the mine and its surroundings has been investigated by Humphrey [1955]. Figure 1, taken from Humphrey's work, shows a map of the mine's 200-foot level and the location of the interferometer. The interferometer is oriented along an axis approximately 7° west of true north.

The interferometer consists of two mirrors of 50-meter radius of curvature and 5 cm diameter. The mirrors are separated by 30 meters and are mounted on piers embedded in bedrock. The mirrors and the optical path between them are enclosed in a vacuum-tight tube which is evacuated to a pressure of approximately 10 millitorr using a conventional mechanical pump. Figure 2 shows the vacuum envelope schematically. Note that the system has been constructed so that no torque or unbalanced force due to atmospheric pressure is exerted on either pier.

The two mirrors are used as a Fabry-Perot interferometer.[1] The intensity of the light transmitted through this type of interferometer is given by

$$I = \frac{I_o}{1 + \frac{4R}{(1-R)^2} \sin^2\left(\frac{2\pi d}{\lambda}\right)} \qquad (1)$$

where R is the power reflectivity of the mirrors, d is the separation

of the mirrors, and λ is the wavelength. (See, for example, Born and Wolf [1970].) The transmission of the Fabry-Perot therefore rises to its maximum value whenever

$$\frac{2\pi d}{\lambda} = n\pi \ , \ n = \text{any integer.}$$

Thus the transmission is a maximum for all wavelengths λ_n for which

$$\lambda_n = \frac{2d}{n}$$

or

$$f_n = \frac{c}{\lambda_n} = \frac{nc}{2d} \qquad (2)$$

The transmission maxima are therefore equally spaced in frequency. The spacing between any two maxima, Δf, is given by

$$\Delta f = f_{n+1} - f_n = c/2d \ .$$

For our case $d = 30$ meters, so $\Delta f = 5$MHz. The full-width at half-maximum of the transmission fringes is easily calculated by setting the denominator of equation 1 equal to 2. We obtain

$$\text{FWHM} = 2f_{1/2} = \frac{c}{\pi d} \sin^{-1}\left(\frac{1-R}{2\sqrt{R}}\right)$$

for the frequency width of the fringes. The finesse of the system is defined to be the ratio of fringe spacing to fringe full-width at half-maximum

$$F = \frac{\Delta f}{2f_{1/2}} = \frac{\pi}{2} \Big/ \sin^{-1}\left((1-R)/2\sqrt{R}\right) \ .$$

For the high reflectivity mirrors typically employed in such interferometry, the arcsine function may be expanded to yield

$$F \simeq \frac{\pi\sqrt{R}}{1-R} \ .$$

Our first interferometer plates were coated to provide a transmission of approximately 3% which would correspond to a theoretical finesse of 104. The measured finesse was 44. The full-width at half-maximum of the transmission bandwidth was therefore only 115 kHz, equivalent to an earth strain of 1.3 parts in 10^9.

The measured finesse of 44 compared with the theoretical finesse of 104 is indicative of an additional 4% power loss per transit, due primarily to absorption and scatter in the multilayer dielectric coating. Recently we have obtained mirror coatings that employ germanium as one of the dielectric layers. While the opacity of this material in the visible region requires a little more experimental skill during the interferometer alignment, its high index of refraction allows coating designs with vastly improved performance at our infrared operating wavelength. We presently have a working finesse of 80, along with 40% transmission coefficient at the interferometric resonance. This corresponds to a reflectivity of 96%, transmission of 1.5%, and an absorption of 1.4% for each mirror. The resulting 62.5 kc fringe width is equivalent to an earth strain of 7 parts in 10^{10}.

Figure 3 shows the transmission fringes obtained for the long-path interferometer, using the original mirrors. Suitable matching optics produce near-perfect single-mode illumination of the long interferometer. This single mode operation is essential if the full sensitivity of the instrument is to be realized and we must therefore discuss it in some detail.

The 30-meter interferometer and the laser which illuminates it, are both examples of curved-reflector Fabry-Perot interferometers. In addition they are termed non-confocal because the mirrors are not separated by their common radius of curvature. The theory of the mode structure of these interferometers has been developed by Fox and Li [1961], and by

Boyd and his co-workers [Boyd and Gordon, 1961; Boyd and Kogelnick, 1962; Boyd, 1964].

Boyd and Gordon [1961] derive an expression for the modes of a non-confocal-spherical-reflector Fabry-Perot. They obtain the resonance condition

$$\frac{4d}{\lambda_{q,m,n}} = 2q + (1+m+n)\left(1 - \frac{4}{\pi}\tan^{-1}\frac{b-d}{b+d}\right)$$

where b is the common radius of curvature of the mirrors and d is their separation. The integer q is the number of axial nodes between the mirrors, m and n denote the number of nodes along two mutually perpendicular transverse axes, and $\lambda_{q,m,n}$ is the wavelength at resonance. In our 30-meter Fabry-Perot, $b = 50$ meters, $d = 30$ meters and so

$$\frac{4d}{\lambda_{q,m,n}} = 2q + (1+m+n)(.689) \quad .$$

The frequencies of these modes will be

$$f_{q,m,n} = c \cdot \frac{1}{\lambda_{q,m,n}} = \frac{c}{2d}\left[q + (1+m+n)(.344)\right] \qquad (3)$$

which is a more exact version of equation 2. As a little algebra will show, the "fundamental" modes, $f_{q,0,0}$ are separated in frequency space by $c/2d$ or 5 MHz. Between these fundamental modes are the so-called off-axis modes. In this calculation m and n are degenerate. Thus $f_{q,0,1}$ and $f_{q,1,0}$ are degenerate in frequency and lie about one-third of the way between two fundamental modes. Likewise $f_{q,1,1}$ lies about two-thirds of the way between two fundamental modes. Furthermore $f_{q,2,1}$ is roughly degenerate with $f_{q+1,0,0}$. This mode structure, which is obtained when the interferometer is illuminated by a non-mode matched source, is clearly visible in Figure 4 which shows the transmission through the 30-meter

interferometer as a function of the incident frequency. We can now appreciate the need for good mode matching. The near-degeneracy of $f_{q+1,0,0}$ with $f_{q,2,1}$ implies that the transmission line shapes of the fundamental modes could be distorted by the presence of the off-axis modes. This distortion would make it more difficult to pick the center of the transmission profile. Thus, any application of interferometry that requires precision definition of line center (such as the present work) will require corresponding care in the selection of cavity configuration and of mode-matching conditions. Before discussing the question of cavity design let us briefly turn to the topic of mode matching.

The eigenmodes of the cavity, with eigenfrequencies $f_{q,m,n}$, have transverse field distributions $T_{q,m,n}$. The transverse field distributions corresponding to the fundamental modes, $T_{q,0,0}$, are Gaussian while the higher order modes have more complicated transverse field distributions. If radiation with some arbitrary transverse field distribution is incident on the cavity, the response of the cavity can be calculated by expanding the incident field in terms of the eigenfunctions of the cavity, $T_{q,m,n}$. The object of mode matching is to reduce this sum to a single term, $T_{q,0,0}$, corresponding to the fundamental lowest order mode with a Gaussian transverse distribution. Due to small departures of the plate figure from perfect sphericity, the experimental "mode" may contain a small admixture of other modes of the ideal resonator. However, it is important to note that the resulting admixture does not degrade the sharpness of the operational resonance response, provided the admixed modes do not themselves have high losses.

The procedure for mode matching may now be formulated explicitly. The lowest order cavity eigenfunctions can be characterized in terms of two parameters: the radius of curvature of the wavefront and the spot diameter. If these two quantities are known at any point in space they

may be calculated at any other point inside or outside of the interferometer. The laser used to illuminate the 30-meter cavity is also a Fabry-Perot interferometer and its output field distribution can therefore also be characterized in terms of a spot diameter and the radius of curvature of the wavefront. The distance between the two cavities is constrained by mechanical limitations. Given the separation between laser and interferometer, the object is to insert optical elements which take the laser spot diameter and radius of curvature and transform them into the cavity spot diameter and radius of curvature, where the mode sizes and radii are both expressed at the same (arbitrary) point. It is intuitively obvious that since two parameters are to be matched, two optical elements (either lenses or mirrors) are, in general, necessary. The solutions are further constrained by the finite number of different components available. The solutions can be most easily found by a "cut-and-try" procedure using, for example, a programmable desk calculator or a time-sharing computer terminal.

We use a two-mirror solution that requires an optical path that is longer than the maximum laser-interferometer separation mechanically allowed and must therefore be "z" shaped.

The design of single-mode cavities for interferometric purposes has been carefully studied by one of us [Hall, 1971]. While the design of the present interferometer was hampered by the limited selection of commercially available mirrors with long radii of curvature, it embodies the most significant design criterion: the first off-axis mode which approaches frequency degeneracy with the dominant modes should be odd symmetric and should have the sum of the off-axis quantum numbers equal to 3 or more. The first criterion comes from the dramatic reduction of the admixture of modes whose transverse quantum numbers sum to an odd integer, since the odd reflection symmetry possessed by these modes is not effectively excited by the symmetric

source function. Thus one may use the first off-axis mode (the "dumbbell" modes, m+n = 1) to very sensitively adjust the laser source to be optically coaxial with the interferometer. The admixture of the "donut" mode (m+n = 2), on the other hand, is very sensitive to the ratio of spot sizes. The ability to independently monitor the spot size ratio and the matching of the radii of curvature contributes to rapid convergence to the proper adjustment. The low admixture exhibited in Figure 3, less than 1/2% of other modes, is preserved for several weeks at a time.

The 30-meter path is illuminated with a helium-neon laser oscillating at 3.39 microns. The laser is RF excited and is approximately 30 cm long. The mirror parameters (60 cm radius vs plane) and the bore diameter (2.3 mm) are carefully chosen to insure that the laser oscillates at a single frequency and in a single spatial mode. One of the mirrors of the laser cavity is mounted on a piezoelectric ceramic. By applying a voltage to this ceramic the laser may be tuned over ± 225 MHz. A small ac dither voltage together with a variable dc voltage are impressed on the piezoelectric crystal. The light transmitted by the long-path interferometer is photoelectrically detected. The resultant signal is amplified and then synchronously detected using the dither frequency as a reference. The output of the synchronous detector, which is proportional to the slope of the Fabry-Perot transmission function, is integrated, filtered, and is then applied to the piezoelectric crystal driver. This servo loop (a "first-derivative" lock) locks the laser to one of the transmission maxima of the long path. When the lock is established the laser's frequency must satisfy equation 2, that is,

$$f_{laser} = \frac{nc}{2d} \quad \text{for some integer } n \ .$$

If the long path changes its length by an amount Δd, the servo will force the laser to change its frequency by an amount

$$\Delta f_{laser} = \frac{-nc}{2d^2} \Delta d$$

so as to keep equation 2 valid. Thus for small changes in length,

$$\frac{\Delta f_{laser}}{f_{laser}} = - \frac{\Delta d}{d} \quad , \qquad (4)$$

so that a measurement of $\Delta f/f$ yields $\Delta d/d$ directly. The laser oscillates at 3.39 microns, so $f_{laser} \approx 1 \times 10^{14}$ Hz and a strain change of 1 part in 10^8 will shift the laser frequency by 1 MHz. Furthermore since only changes in laser frequency are significant, the same result would be obtained using equation 3 instead of equation 2 for the eigenfrequencies.

Analysis of the theory of servo mechanisms shows that one cannot build the servo loop described above to have arbitrarily wide frequency response. In other words, a finite time is required to make a frequency correction. It is useful to characterize the servo system in terms of its response to a unit step. The experimental response to such an input is shown in Figure 5. It can be seen that the system requires about 1½ milliseconds to make a correction, corresponding to a bandwidth of well over 100 Hz. A servo-loop slope of 9 db/octave (= 30 db/decade) is employed. The dc loop gain of 120 db yields completely negligible static errors.

To guarantee the proper operation of the servo system, the laser's frequency must vary monotonically with the voltage applied to the piezoelectric ceramic. This may not be true if any light is reflected back into the laser from the Fabry-Perot. Even a small amount of reflected power can pull the laser frequency by a surprisingly large amount. Elementary calculations suggest that a reflected power of only 1 part in 10^5 of the incident power will pull the laser frequency by about 1 part in 10^8. (For details, see Boyne, et al. [1970].) This effect, which is well known in the behavior of coupled, tuned, electronic circuits, has apparently been overlooked by several workers in the laser strainmeter

field. The fringe distortion and frequency "hang up" that result from using inadequate reverse decoupling can be easily demonstrated.

In Figure 6a the upper trace shows the transmission intensity of the long-path interferometer. The lower trace shows the oscillation frequency of the laser. The x axis of the oscilloscope is driven from the voltage applied to the piezoelectric ceramic on the laser. Note that the fringes are symmetric and that the laser's frequency varies smoothly as we sweep through a fringe.

In Figure 6b we have reduced the decoupling between laser and interferometer so that the return light from the interferometer is only attenuated by about 10 db. Note that the fringes have now become strongly asymmetric and that the transmission intensity has a tendency to "snap" as the center of the fringe is reached. Furthermore, note that at the center of the fringe the laser's oscillation frequency "hangs up" even though the piezoelectric crystal continues to move the mirror. Needless to say, both of these effects play havoc with the servo systems.

However, the "hang up" and the "snap" are not the saddest parts of the story. When the decoupling is inadequate the laser's oscillation frequency is determined by the sum of the cavity field at the output mirror and the field returned from the interferometer. The resultant field depends on the relative phase between these two fields. The phase in turn depends not only on the phase shift in the long-path interferometer but also upon the optical path between the laser and interferometer. This optical path is on the order of 1 meter or about 300,000 wavelengths. Thus a change in the index of refraction of 1 part per million will change the relative phase of the return beam by π radians which will generate

an enormous change in the laser's oscillation frequency. The frequency shift depends on the intensity of the reflected power and can easily be on the order of megahertz. Shifts of this magnitude are equivalent to earth strains of several parts in 10^8. Such index of refraction changes can be generated by temperature fluctuations on the order of 1°C. We conclude that in addition to "snap" and "hang up" the system becomes sensitive to small changes in temperature and atmospheric pressure.

The system would also be sensitive to small changes in the physical distance between laser and interferometer. If any of the mirrors move by as little as 3/4 micron the return signal will change phase by π radians. The conclusion is that good isolation is essential not only for good line profiles but for stable laser oscillation as well. It is clear that the same kind of considerations apply to lower finesse interferometers (such as Michelson's) and to systems which measure the fringe position rather than track it dynamically.

To achieve adequate isolation we have used an optically excellent linear polarizer (Rochon prism) followed by an adjustable crystal quartz quarter wave plate between the laser and the long path. When this system is properly adjusted, there is no observable frequency "hang up" as the laser is tuned through a long-path fringe. See Figure 6a. An additional multiplicative isolation of 30 db is available using an yttrium iron garnet (YIG) crystal as a Faraday isolator [Gamo et al., 1967].

Optical Reference Laser. The reference frequency for the system is provided by a second, independent 3.39 micron laser that is locked to a molecular absorption frequency in methane. This laser, developed by R. L. Barger and J. L. Hall, has been described in detail in the literature and will be only briefly described here [Barger and Hall, 1969].

A laser cavity is constructed containing a helium-neon gain cell and an absorption cell filled with methane to a pressure of about 12 millitorr. A quantitative analysis of this problem is extremely complicated, but a simple physical model analogous to the model of the Lamb dip [Bennett, 1962, 1970] contains the essential ideas. The helium-neon cell can provide gain over a relatively wide range of frequencies given by the Doppler width of the neon line in question. This width is on the order of 360 MHz. By properly constructing the cavity so that only one sufficiently high-Q mode lies within the Doppler profile, the laser can be forced to operate on a single frequency. A standing wave will be set up in the cavity. This can be thought of as two running waves in opposite directions. If this frequency of oscillation does not correspond to the methane absorption frequency, only those methane molecules whose velocity down the cell axis is high enough to provide the requisite Doppler shift will absorb the radiation. The two running waves will be absorbed by two different velocity groups which will cause two holes to be burned in the velocity distribution of methane molecules in the state that absorbed the energy. As the oscillation frequency is brought closer and closer to the methane line center, methane molecules with smaller and smaller Doppler shifts are excited until, at the center of the methane line, only those molecules with no Doppler shift are excited. At this point both running wave fields will be "pumping out" the absorbing molecules that have the right velocity component, namely zero, along the laser axis. This resulting extra depletion of methane molecules reduces the intracavity absorption at molecular line center and therefore results in increased laser output power at this frequency. Figure 7 shows this phenomenon superimposed on the methane laser's Doppler profile. By dithering one of the mirrors of the methane laser cavity, it is possible

to lock the methane laser's frequency to the peak of the emission feature using the "first derivative lock" described above.

A portion of the output of the methane-stabilized 3.39 micron laser is heterodyned in a fast indium arsenide diode with part of the output of the laser locked to the long path. The diode mixes the two signals and generates, among other signals, a signal at the difference frequency between the two lasers.

The mixing results from the fact that the diode responds not to the incident electric field but to the incident intensity, which is proportional to the field squared. Thus the output of the diode is proportional to $(E_{Lp} + E_{methane})^2$ where E_{Lp} and $E_{methane}$ are the optical fields incident on the diode from the laser locked to the long path and the methane-stabilized laser respectively. If

$$E_{Lp} = E_0 \cos(\omega_0 t + \phi_0)$$

$$E_{methane} = E_1 \cos(\omega_1 t + \phi_1)$$

then the diode will have a component of its output of the form

$$A \cos\left[(\omega_0 - \omega_1)t + (\phi_0 - \phi_1)\right] .$$

Inspection of this formula shows that it is not trivial to obtain a beat signal. The diode has an active area that is many wavelengths in diameter. If the quantity $\phi_0 - \phi_1$ varies appreciably across the active area of the diode, different parts of the diode's surface will generate beat signals with differing phases and these contributions to the beat signal will interfere. This interference must reduce the beat signal's amplitude relative to what it would have been had $\phi_0 - \phi_1$ been constant across the active area of the diode. Thus a failure to keep

$\phi_0 - \phi_1$ constant will result in a reduction of the signal-to-noise ratio in the beat circuit.

A moment's thought will show that a necessary and sufficient condition for $\phi_0 - \phi_1$ to be constant across the diode is for the two beams to be colinear and for the radii of curvature of the two beams to be the same. In addition it would be desirable, although not essential, for the two beams to be of the same diameter. It is clear that the techniques for satisfying these criteria are the same as those used to obtain mode matching of two cavities as described above. However, the requirements here are not quite as stringent since imperfect mode matching degrades the signal-to-noise ratio in the beat circuit, and therefore the maximum detectable beat frequency, but does not introduce any systematic problems in the measurement at any one frequency.

Since

$$f_{beat} = f_{long\ path} - f_{methane}$$

$$\frac{\Delta f_{beat}}{f_{long\ path}} = \frac{\Delta f_{long\ path}}{f_{long\ path}} - \frac{\Delta f_{methane}}{f_{long\ path}}$$

$$= -\frac{\Delta d}{d} - \frac{\Delta f_{methane}}{f_{long\ path}} \quad . \qquad (5)$$

If we postpone for a moment a discussion of $\Delta f_{methane}$ [we will show it to be essentially zero] then

$$\frac{\Delta f_{beat}}{f_{long\ path}} = -\frac{\Delta d}{d}$$

so that a measurement of the fluctuations of the beat frequency is a direct measurement of the strain change in the long path. Figure 8 shows the strainmeter schematically.

Data Recording. The data output of the strainmeter consists of the beat frequency, which is sampled at regular intervals. The frequency samples are digitally recorded on standard 7-track computer magnetic tape together with time-of-day information. These samples may then be plotted, digitally filtered, or Fourier transformed. The results of such analyses will be presented in detail in a subsequent paper.

SENSITIVITY OF THE SYSTEM

The useful sensitivity of this system to strains of geophysical interest is limited in two different ways. Firstly we must investigate the limits placed on the system by systematic and random errors within the interferometer and its associated electronics. Secondly we must consider the possibility that an incident seismic disturbance is altered by the local geology and/or by the piers before it reaches the interferometer.

The system noise can be attributed to two main sources. First is the noise in the methane-stabilized laser. From equation 5 it is clear that any fluctuations in the methane laser's frequency produce first-order changes in the beat frequency. The stability of the methane laser is being investigated by R. L. Barger and J. L. Hall. They have constructed two such lasers and have monitored the fluctuation in their difference frequency as a function of time. Their results are presented in Figure 9 which shows the Allen variance function of the beat frequency between two independent devices as a function of the measurement (averaging) time. The Allen variance measures the average fractional difference between two adjacent samples of the beat frequency between two coherent sources as a function of the sampling time. This function proves to be very useful in the frequency standards field, largely because it remains well

defined even in the presence of noise with long time correlation, such as noise with a "1/f" spectral distribution. The Allen variance contains roughly the same information as a Fourier transform, although with substantially less detail.

Note that for times less than about 100 sec the frequency fluctuations decrease in a manner consistent with the hypothesis that the noise source is approximately white. It can be seen from Figure 9 that for the usual times of geophysical interest ($t > 100$ msec) the methane laser's frequency fluctuates by a few parts in 10^{12} or less. An independent reproducibility better than 1×10^{-11} was demonstrated in the early experiments. Work on the methane-stabilized laser device is continuing and the results presented here should not be regarded as the ultimate attainable with this system: stability levels approaching 10^{-14} have already been achieved with somewhat more sophisticated laser devices.

The second important source of instrumental noise is the fluctuation of the long-path servo lock. With the first set of mirrors, the signal-to-noise ratio in the long-path lock was of order 50 to 1 in a 20 kHz bandwidth. If we pick 1 msec as a desirable servo attack time, the signal-to-noise ratio is increased by a factor of 11 (by the resulting integration) to a factor of 550 to 1. Thus, using the transmission function of equation 1, this servo will have a noise level of less than 3×10^{-3} linewidths for a 1 msec integration. For our 115 kc fringe linewidth, we thus obtain less than 350 Hz equivalent rms frequency noise. The corresponding apparent geophysical strain noise is less than 4×10^{-12} decreasing at 6 db/octave for integration times longer than 1 msec. The power spectrum has not yet been completely measured, but preliminary measurements show that in the frequency range of 1 to 5 Hz, the total system noise (that is,

the noise of the methane laser plus the noise of the long-path lock) is less than, or equal to, 2 parts in 10^{13} per unit bandwidth. Again, this figure should not be regarded as the ultimate attainable with this system, particularly in view of the dramatically improved new mirror coatings. Servo loop gains of 120 db reduce the static loop errors to insignificant levels.

Thus we can conclude that the optical/electronic system is capable of measuring the effective interferometer length with very high precision. It is therefore of interest to investigate the relationship between the observable, the interferometer length, and the interesting physical variable, one component of the earth strain tensor.

We consider first the piers on which the interferometer is mounted and the rock formations in the immediate vicinity of the interferometer. We can distinguish three different classes of problems that might arise: (1) The piers (and by piers we shall henceforth mean the piers and the rock immediately adjacent to them) may exhibit a non-uniform transmission as a function of frequency. That is, the piers may enhance disturbances at certain frequencies because of mechanical resonances. (2) The piers may exhibit a slow creeping with time. (3) The piers may exhibit non-elastic behavior or hysteresis whereby large disturbances produce permanent offsets in the length of the interferometer.

To investigate these possibilities we have performed two experiments. The first is a measurement of the impulse response of the system. A "seismic disturbance" is generated by striking the tunnel wall with a 10 kg sledge hammer. The energy imparted by the blow is on the order of 180 J. Figure 10 shows the response of the system when the blow is struck on the tunnel wall approximately halfway between the two piers. Note that the

system responds elastically, exhibiting no permanent offset or hysteresis. Furthermore the system shows no strongly resonant behavior and transmits frequencies from dc up to the Nyquist limit of the display (50 Hz since the sampling rate is 10 msec). In fact higher frequencies are also present but have been aliased by the 10 msec sampling rate. The system does exhibit a weak resonance at about 34 Hz with a Q of about 40. We have repeated this measurement 8 times, striking the wall at a different point each time. The distance from the point of impulse to the interferometer was varied from halfway between the piers to 45 m away from the interferometer. In addition the angle between the interferometer axis and a line from the point of impact to the interferometer was varied from 0° to almost 90°. In this way the response of the instrument to signals coming from different directions could be surmised.

The results of these experiments were not very surprising. The Gold Medal reef (see Fig. 1) serves as a low-pass filter and heavily attenuates seismic disturbances above about 50 Hz passing across it. In addition the interferometer is most sensitive to signals incident along its axis and is essentially insensitive to signals incident at 90° to its axis.

These results are not meant to be exciting. Rather they attempt to show that the interferometer is not located in an area which has large local anomalies in its seismic properties. So far as we can determine, the local geology has essentially no hysteresis or other non-elastic behavior and does not show any strong resonances in its transmission of seismic signals.

We have also investigated the possibility of creep in the piers or a gradual strain change in the surrounding rock. We have monitored the earth tides for 42 days (1008 hours). Most of these data will be discussed in greater detail in the next section. We will show there that the average

baseline drift over this period was $0 \pm 1 \times 10^{-10}$ per day. This figure is degraded somewhat during the spring thaw when the mine becomes partially flooded. During this period secular strains of 5 ± 10^{-9} per day have been recorded.

ADVANTAGES OF THE SYSTEM AND SOME GEOPHYSICAL RESULTS

From the foregoing discussion, it is clear that the methane-stabilized laser strainmeter possesses unique advantages over conventional instruments. First, it has a uniformly high sensitivity over its wide bandwidth. This, coupled with its good long-term stability, allows the same instrument to be used for studying long-term changes in the strain field, rock tides, and the relatively high frequencies associated with seismic events.

Second, the data output is a frequency rather than a voltage and is therefore inherently free from the problems of analog electronics. In addition, the data are in a computer-compatible format which facilitates subsequent processing.

Third, the earth strain is measured digitally in terms of precision quartz crystal oscillators and therefore problems with mechanical calibration devices do not arise. The drift of the reference laser frequency has been shown to be completely insignificant on the sensitivity scale of interest geophysically.

To illustrate the wide bandwidth of the instrument, in Figure 11 we show the seismic signal generated by the nuclear explosion Boxcar, a one-megaton device detonated at the Nevada test site on 26 April, 1968. The record represents the first 11 sec of the seismic signature. The first arrival has a rise time of about 0.22 sec and represents a strain change of about 6 parts in 10^{11}. The signal-to-noise ratio in the first step

is about 11 db. From Figure 5 it is clear that the rise time of the first arrival is not the instrumental step response. To a first approximation it represents the convolution of the impulse response of the seismic path between the test site and Boulder with the source function of the blast. This greatly complicates the identification of the source when data are available from only one station. Nevertheless, seismic discrimination for a relatively large event seems to be possible using only the data from a single station. This can be done by computing the power spectrum of the first 3 sec of the data and comparing it with the power spectrum in the subsequent 15 sec. The ratio of these two power spectra is similar to the "complexity" discriminant discussed by Evernden [1969]. It is clear that this technique must fail for sufficiently distant and/or sufficiently weak signals but we do not have enough data to set any limits on the usefulness of the technique.

CONCLUSIONS

We have constructed a laser strainmeter with several important advantages over conventional mechanical and laser-optical instruments. We have illustrated the system's capabilities using several different types of experiments. We are continuing to improve the system's sensitivity and reliability.

ACKNOWLEDGMENTS

We are pleased to acknowledge the many helpful discussions we have had with the following people during the course of this work: Dr. Peter Bender of JILA, Dr. J. C. Harrison and Dr. W. E. Farrel of the Cooperative Institute for Research in the Environmental Sciences of the University

of Colorado, Boulder, Colorado, Dr. F. Gilbert and Dr. J. Berger of the Institute for Geophysics and Planetary Physics, University of California, San Diego, California, and Dr. M. W. Major of the Colorado School of Mines, Golden, Colorado.

REFERENCES

Barger, R. L., and J. L. Hall, Pressure shift and broadening of methane line at 3.39 microns studied by laser-saturated molecular absorption, Phys. Rev. Letters, 22, 4, 1969.

Bennett, W. R. Jr., Hole burning effects in a He-Ne optical maser, Phys. Rev., 126, 580, 1962.

Bennett, W. R. Jr., Hole burning effects in gas lasers with saturable absorbers, Comments on Atomic and Molecular Physics, 2, 10, 1970.

Born, M., and E. Wolf, Principles of Optics, 4th edition, p. 329ff., Pergamon Press, London, 1970.

Boyd, G. D., and H. Kogelnick, Generalized confocal resonator theory, Bell System Techn. J., 41, 1347, 1962.

Boyd, G. D., and J. P. Gordon, Confocal multimode resonator for millimeter through optical wavelength masers, Bell System Tech. J., 40, 489, 1961.

Boyd, G. D., Modes in confocal geometries, in Quantum Electronics III, edited by P. Grivet and N. Bloembergen, Columbia University Press,, New York, 1964.

Boyne, H. S., J. L. Hall, R. L. Barger, P. L. Bender, J. Ward, J. Levine, and J. Faller, Absolute strain measurements with a 30-meter interferometer, in Laser Applications in the Geosciences, pp. 215 ff., Western Periodicals, North Hollywood, California, 1970.

Evernden, J. F., Identification of earthquakes and explosions by use of teleseismic data, J. Geophys. Res., 74, 3828, 1969.

Fox, A. G., and T. Li, Resonant modes in a maser interferometer, Bell System Tech. J., 40, 453, 1961.

Gamo, H., S. C. Chuang, and R. E. Grace, Infrared isolator using yttrium iron garnet, IEEE J. Quantum Electron., QE-3, 243, 1967.

Hall, J. L., Laser wavelength standards, saturated molecular absorption and high precision length metrology, 1971 (to be published).

Humphrey, A. G. Jr., The geology of Poorman Hill and the Poorman Mine, Boulder County, Colorado, M. S. thesis, University of Colorado, 1955 (unpublished).

Figure Captions

Figure 1. The geology of the 200 foot level of the Poorman's Relief Mine, Boulder County, Colorado.

Figure 2. Details of the vacuum envelope of the laser interferometer.

Figure 3. The fundamental transmission fringes of the 30-meter interferometer using the original 97% reflectivity mirrors. The x-axis of the oscilloscope is driven from the voltage applied to the piezoelectrically drived mirror on the laser illuminating the interferometer and is proportional to the frequency of the light incident on the interferometer (vide infra). The y axis is driven from the photoelectric detector placed at the far end of the interferometer. The y axis sensitivity is 50 μW/cm.

Figure 4. The transmission fringes of the 30-meter interferometer showing the fundamental and off-axis modes. Except for the halving of the y axis sensitivity (to 100 μW/cm) the display is produced the same way as in Figure 3.

Figure 5. Step response of the long-path servo lock. The x axis sweep speed is 500 μsec/cm. The y axis shows the error signal in the servo resulting from a step voltage applied to the piezoelectric tuning crystal in the laser illuminating the long path.

Figure 6. (a) Upper trace: y axis driven from power transmitted through 30-meter interferometer; lower trace: y axis signal is proportional to the laser's oscillation frequency. This signal is obtained by heterodyning the laser in question with a second 3.39 micron laser with good short term stability. The re-

sulting radio-frequency beat is then converted to a voltage with a scale factor of 1 volt/MHz. The common x axis drive is derived from the piezoelectric tuning voltage being applied to the laser illuminating the long path.

(b) This figure is obtained using the same system as in (a) except that optical decoupling between laser and interferometer has been reduced so that the return light is only attenuated by about 10 db.

Figure 7. The principle of saturated absorption. The figure shows the output power of a 3.39 micron helium-neon laser with a methane cell inside the cavity as a function of cavity length. Note the sharp emission feature superimposed on the Doppler profile of the laser's output power. The dc output power is about 300 μW and the emission feature is about 3% of this. (The displacement of the two traces is due to hystersis in the piezoelectric crystal.)

Figure 8. Block diagram of the 30-meter laser interferometer.

Figure 9. The Allen variance of the methane stabilized laser. It is computed by measuring the average fluctuation of the beat frequency between two independently stabilized lasers as a function of the averaging time. The variance is then expressed as the ratio of these quantities to the output frequency which is on the order of 10^{14} Hz.

Figure 10. The "impulse response" of the system. This shows the response of the system to striking the tunnel wall with a 10 kg sledgehammer midway between the piers. The beat frequency

was sampled 100 times per second and the resulting samples were plotted with no adjustments. The scales are ±100 parts in 10^{12} on the y axis and 0-4 seconds on the x axis.

Figure 11. First motion of the nuclear explosion Boxcar, detonated at the Nevada Test site on 26 April 1968. The record shows the first 11 sec of the seismic signal. The data have not been filtered but a least-squares-fitted straight line has been subtracted prior to plotting.

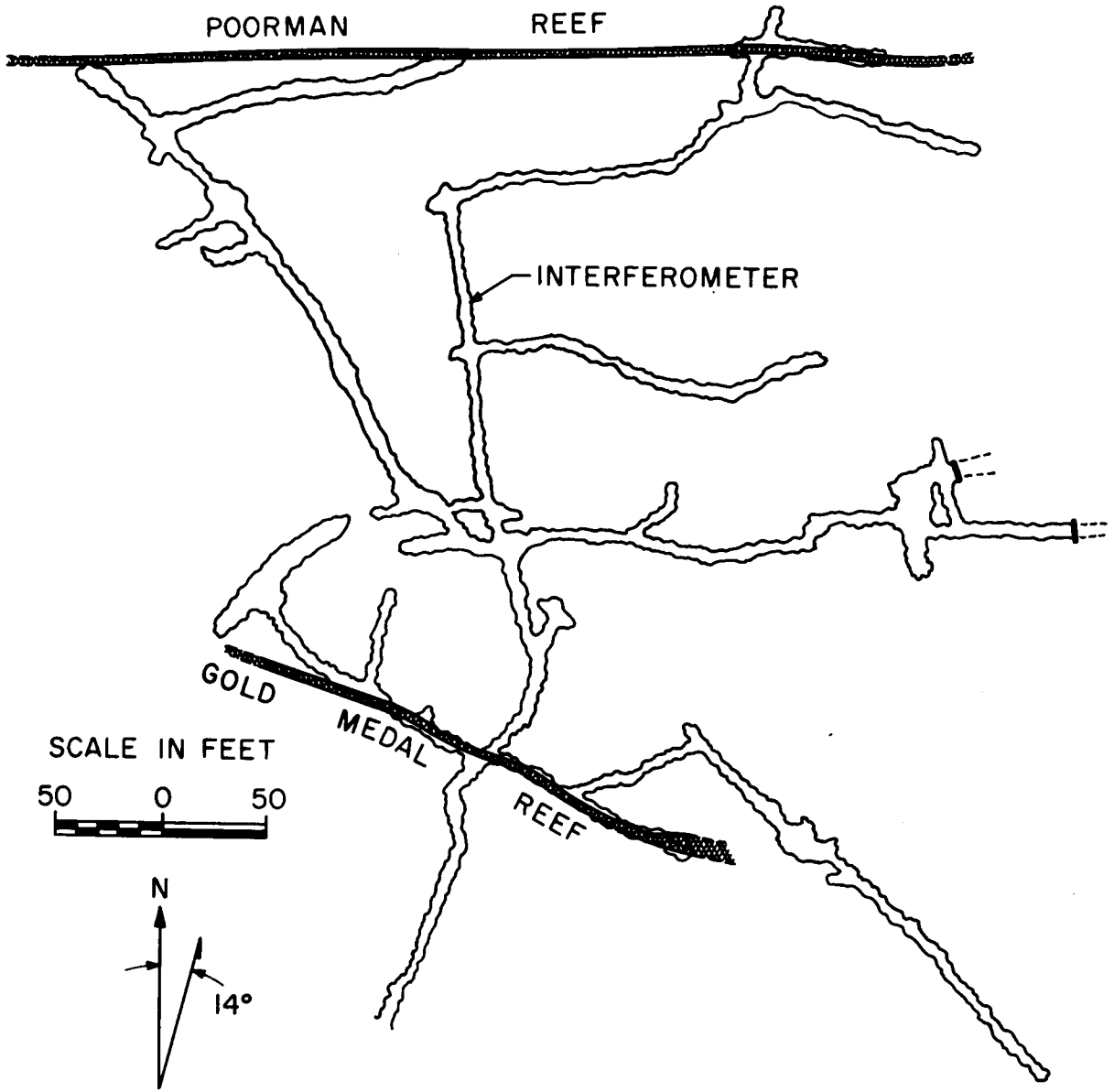
POORMAN
REEF
INTERFEROMETER
GOLD
MEDAL
REEF
SCALE IN FEET
50
0
50
N
14°

Fig. 1

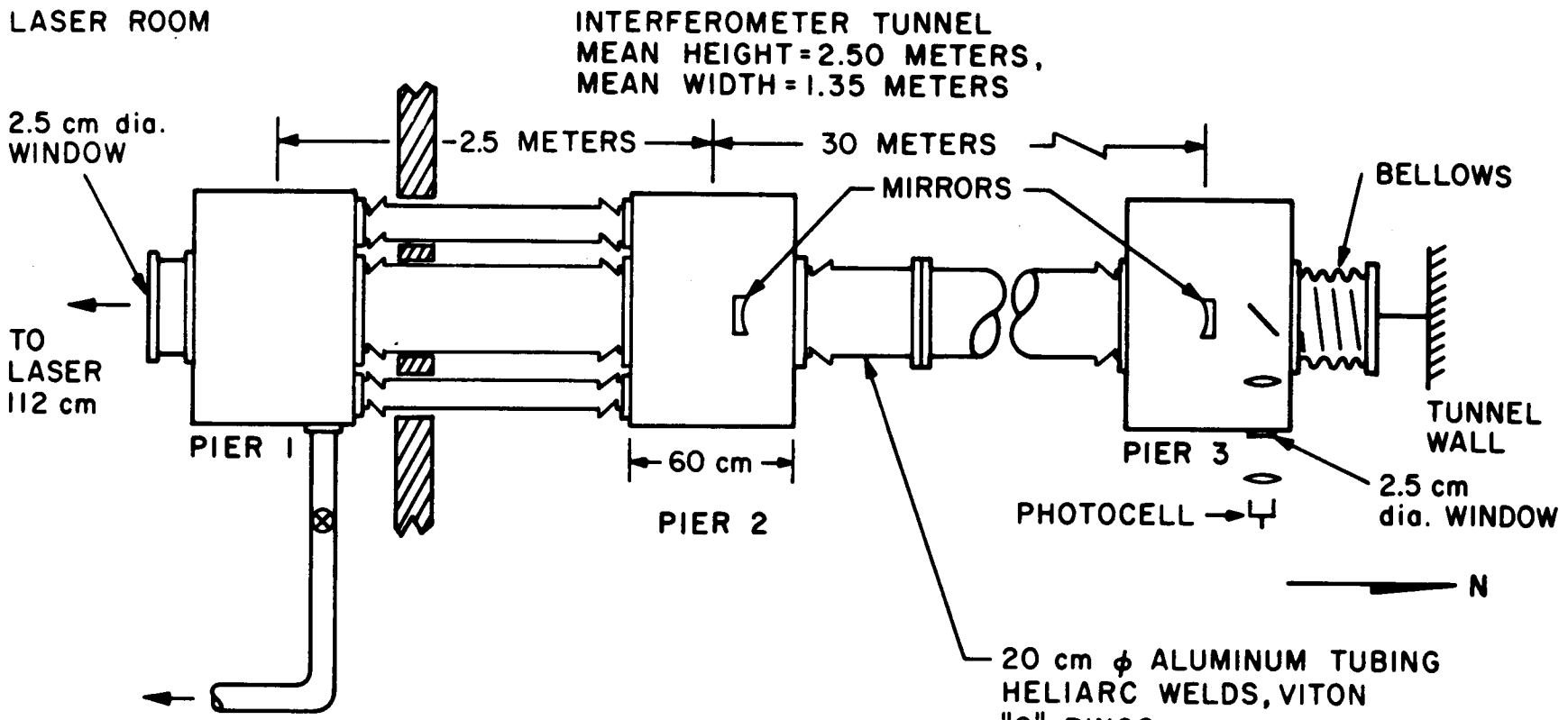

NOTE: PIER 1 IS NOT USED
THE MIRRORS ARE MOUNTED ON PIERS 2 AND 3 AS SHOWN
THE ALIGNMENT MAY BE ADJUSTED WHILE THE SYSTEM IS EVACUATED
THE DRAWING IS NOT TO SCALE

VACUUM ENVELOPE AT POORMAN MINE

Fig. 2

95671

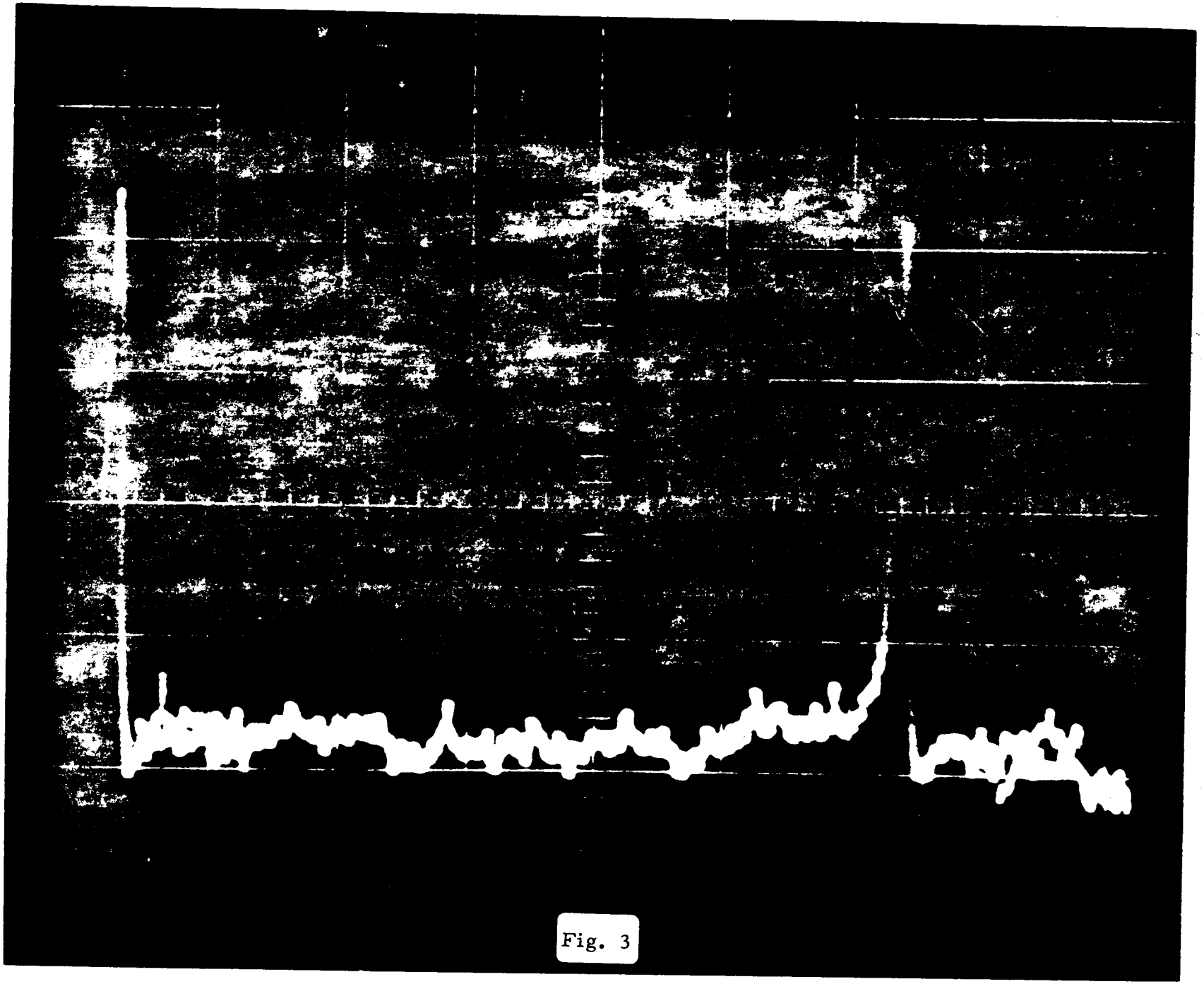

Fig. 3

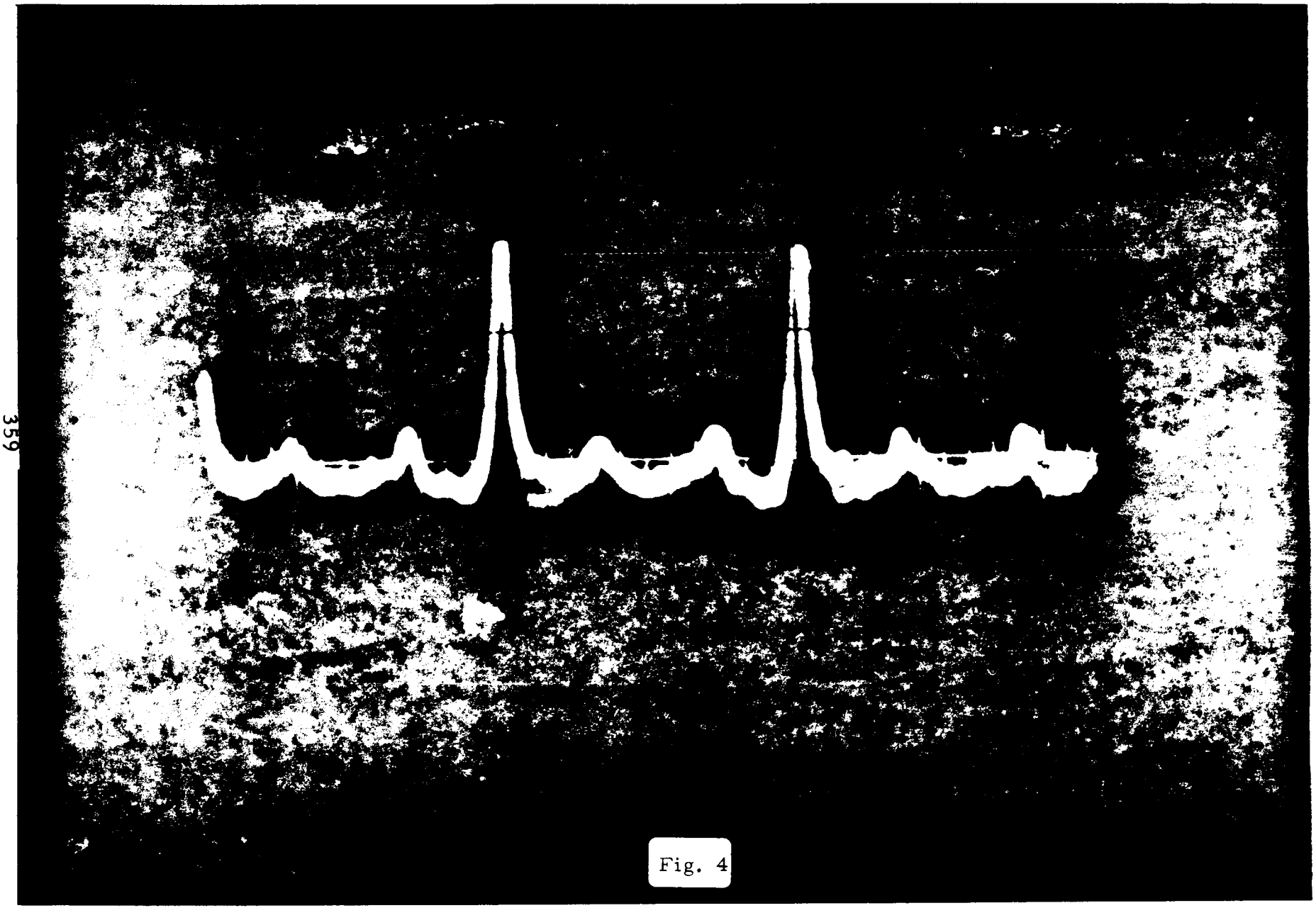

Fig. 4

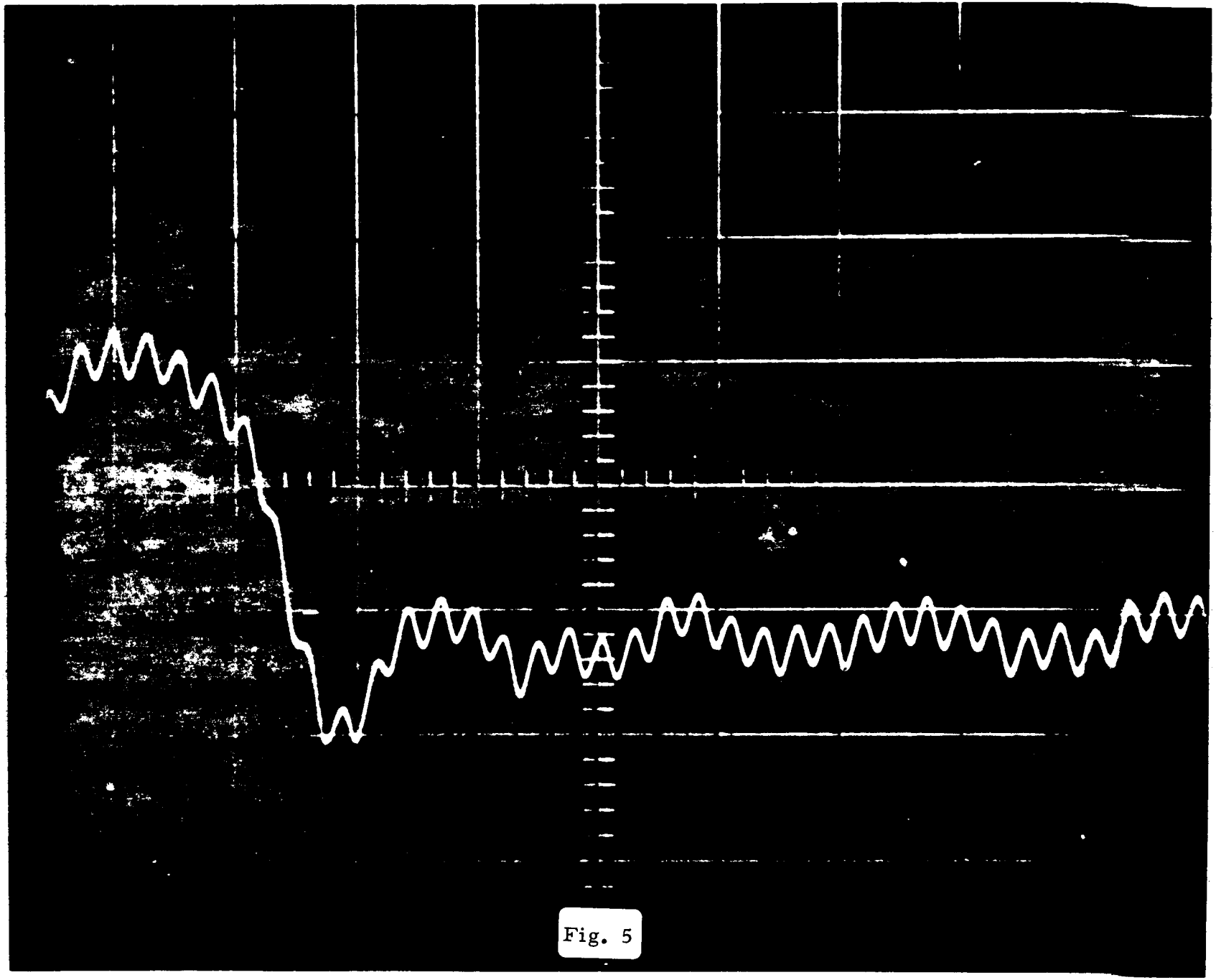

Fig. 5

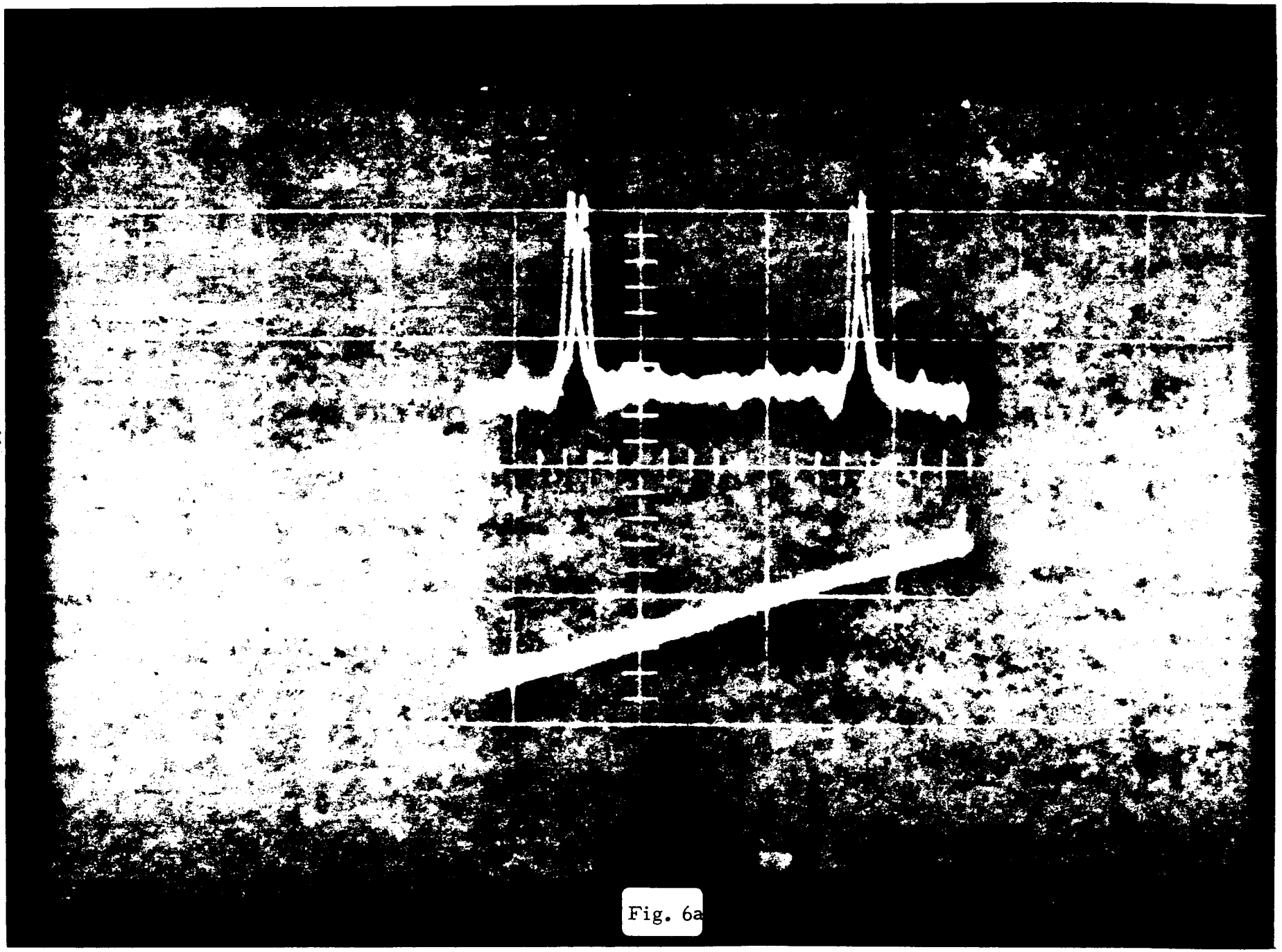

Fig. 6a

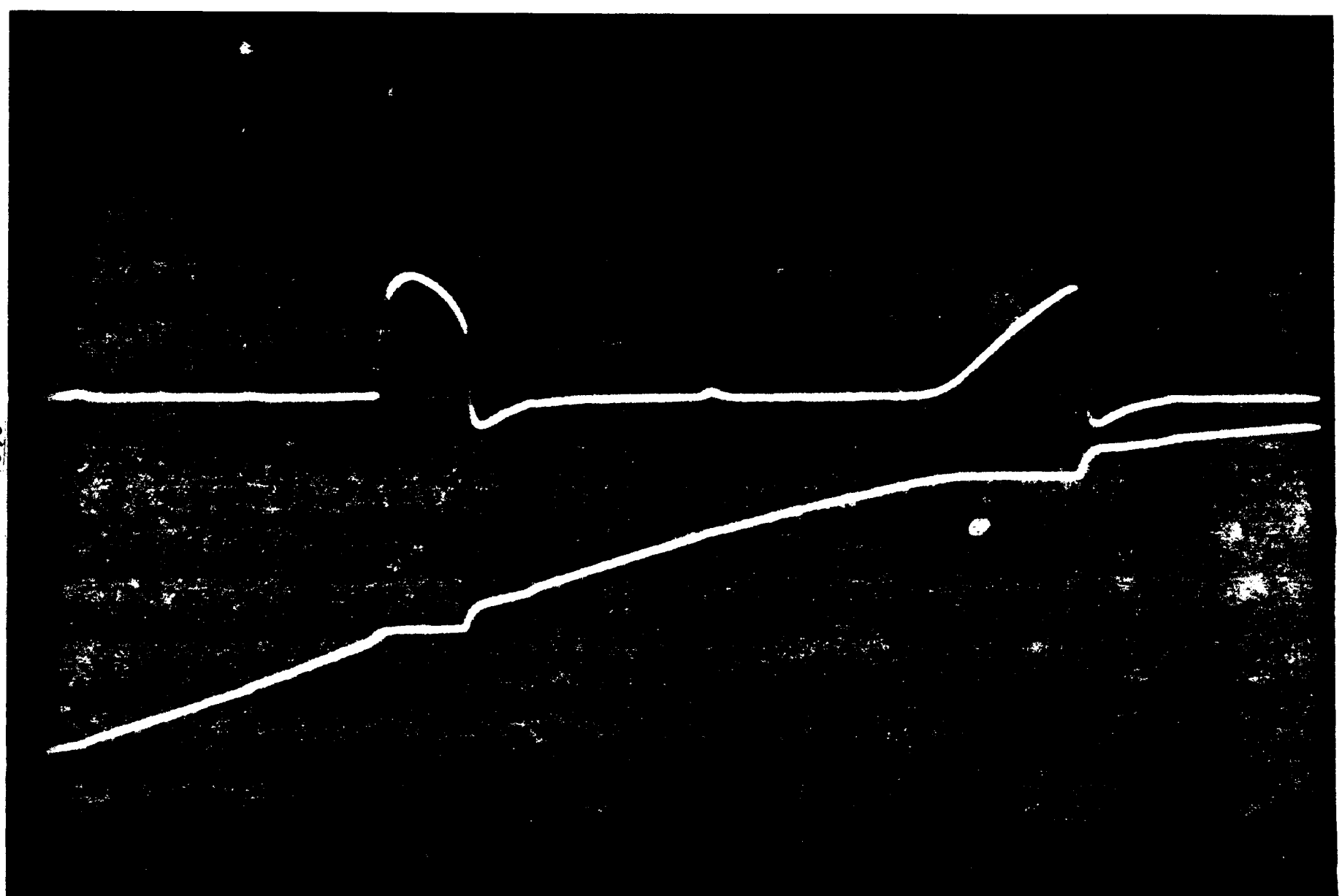

Fig. 6b

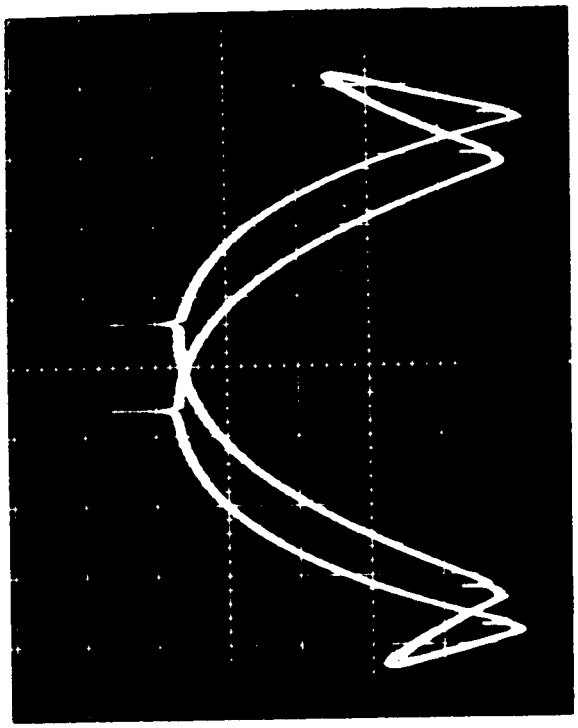

Fig. 7

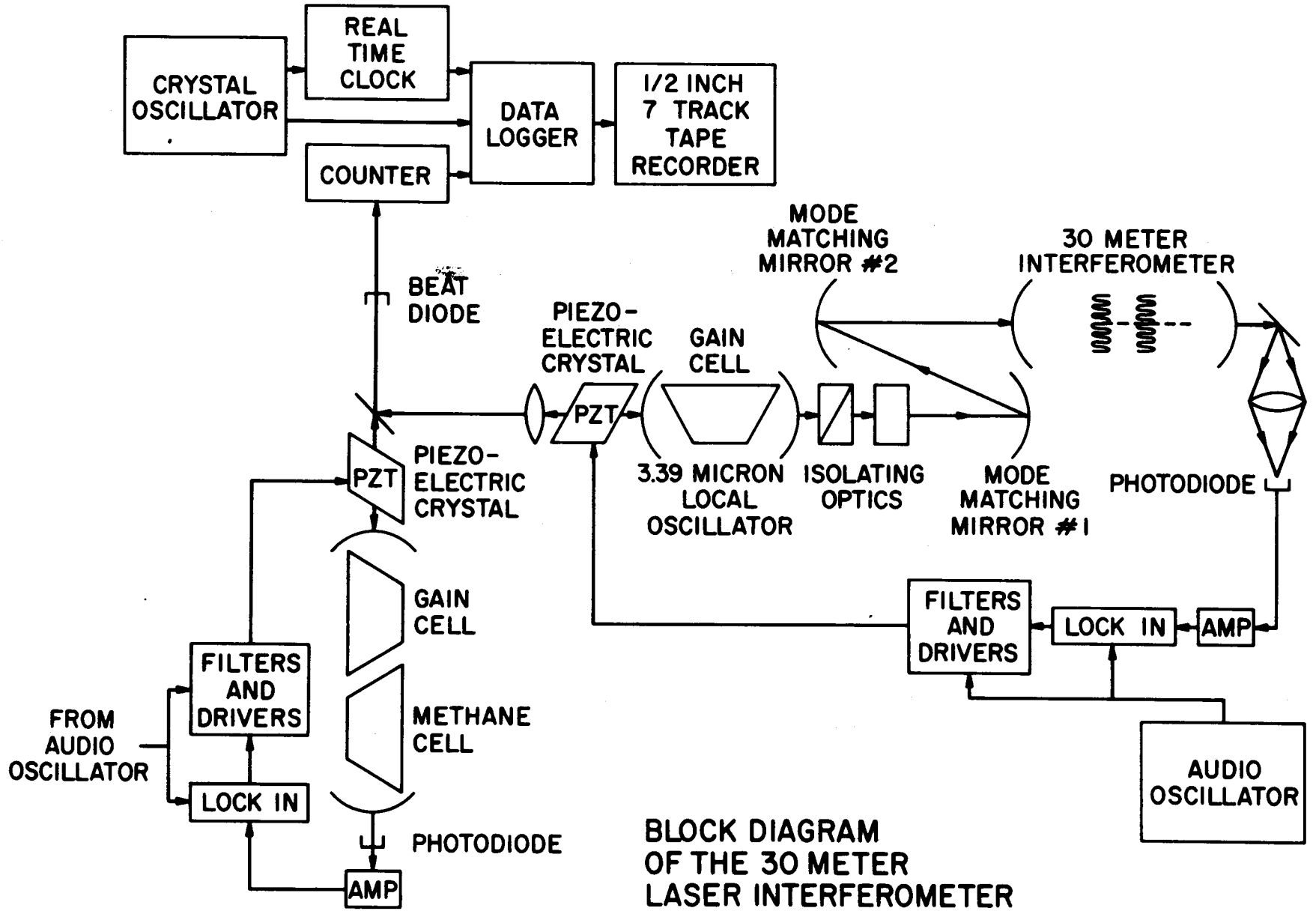
REAL TIME CLOCK
CRYSTAL OSCILLATOR
DATA LOGGER
1/2 INCH 7 TRACK TAPE RECORDER
COUNTER
MODE MATCHING MIRROR #2
30 METER INTERFEROMETER
BEAT DIODE
PIEZO-ELECTRIC CRYSTAL
GAIN CELL
PZT
PIEZO-ELECTRIC CRYSTAL
3.39 MICRON LOCAL OSCILLATOR
ISOLATING OPTICS
MODE MATCHING MIRROR #1
PHOTODIODE
GAIN CELL
FILTERS AND DRIVERS
LOCK IN
AMP
FROM AUDIO OSCILLATOR
FILTERS AND DRIVERS
METHANE CELL
LOCK IN
AUDIO OSCILLATOR
PHOTODIODE
AMP
BLOCK DIAGRAM OF THE 30 METER LASER INTERFEROMETER

Fig. 8

95672

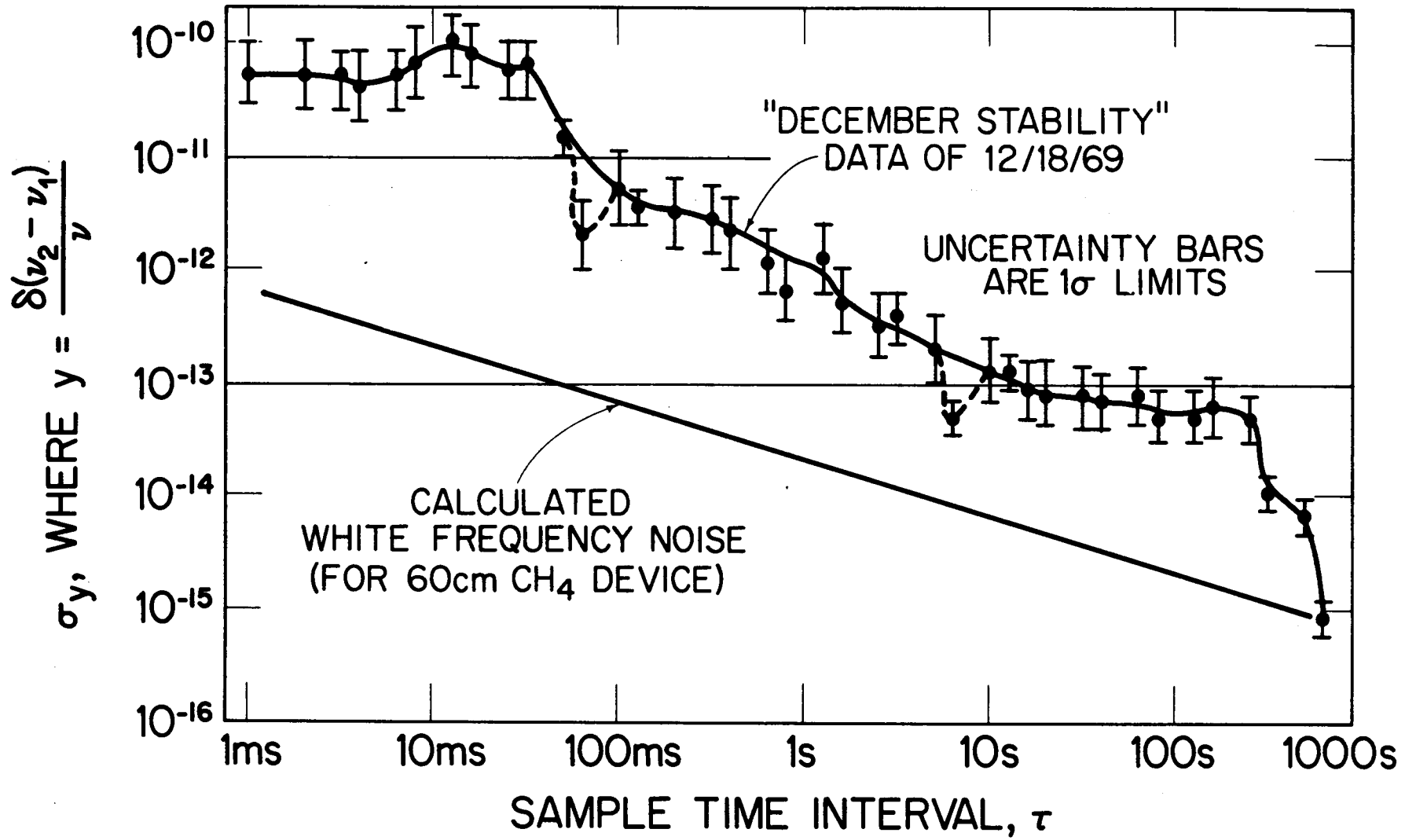
σ_y, WHERE $y = \frac{\delta(\nu_2 - \nu_1)}{\nu}$
10^{-10}
10^{-11}
10^{-12}
10^{-13}
10^{-14}
10^{-15}
10^{-16}
"DECEMBER STABILITY"
DATA OF 12/18/69
UNCERTAINTY BARS
ARE 1σ LIMITS
CALCULATED
WHITE FREQUENCY NOISE
(FOR 60cm CH_4 DEVICE)
1ms
10ms
100ms
1s
10s
100s
1000s
SAMPLE TIME INTERVAL, τ

Fig. 9

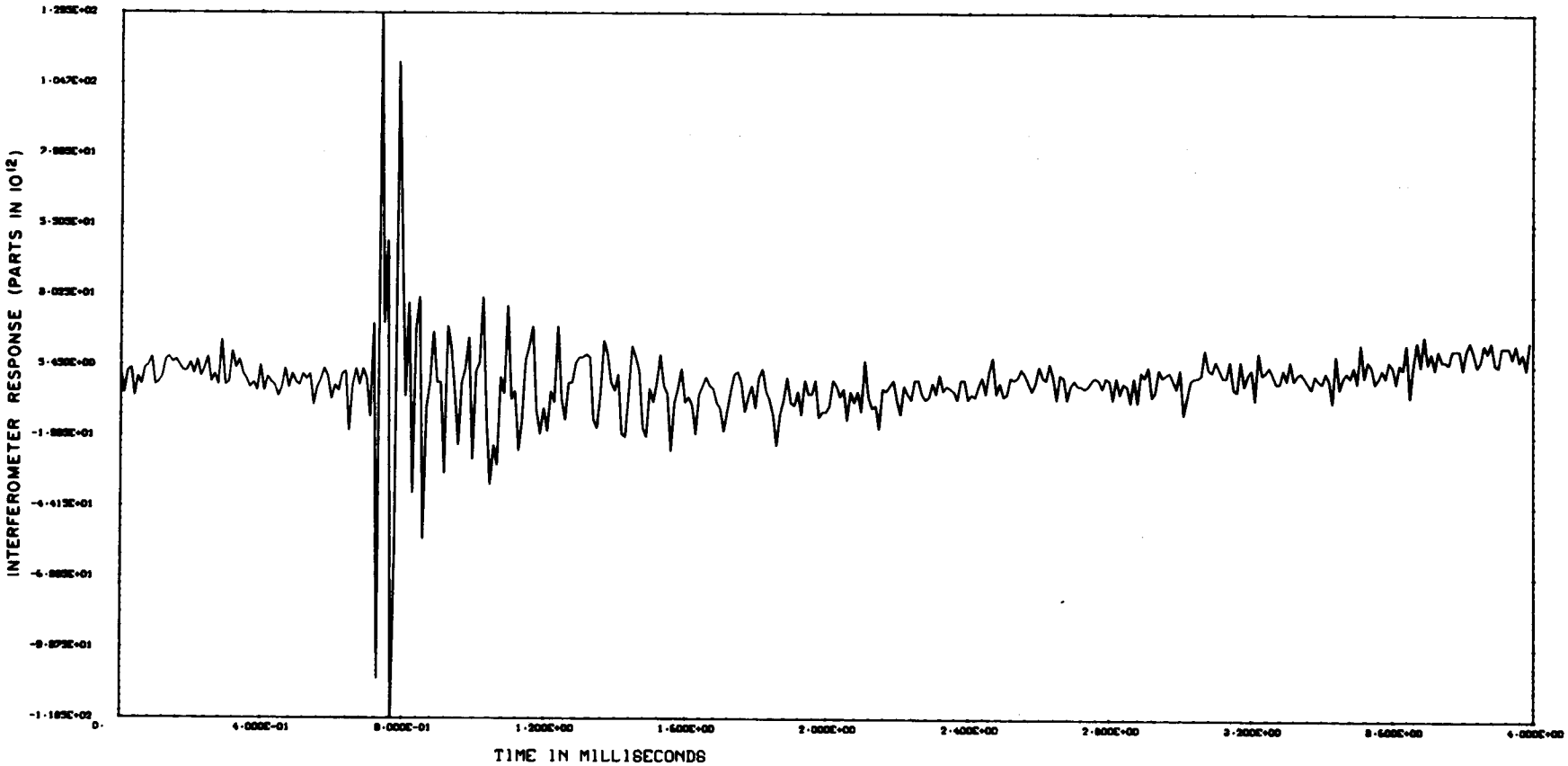
INTERFEROMETER RESPONSE (PARTS IN 10¹²)
TIME IN MILLISECONDS
IMPULSE RESPONSE OF LONG PATH 6 MAY 71 10 MSEC/SAMPLE

Fig. 10

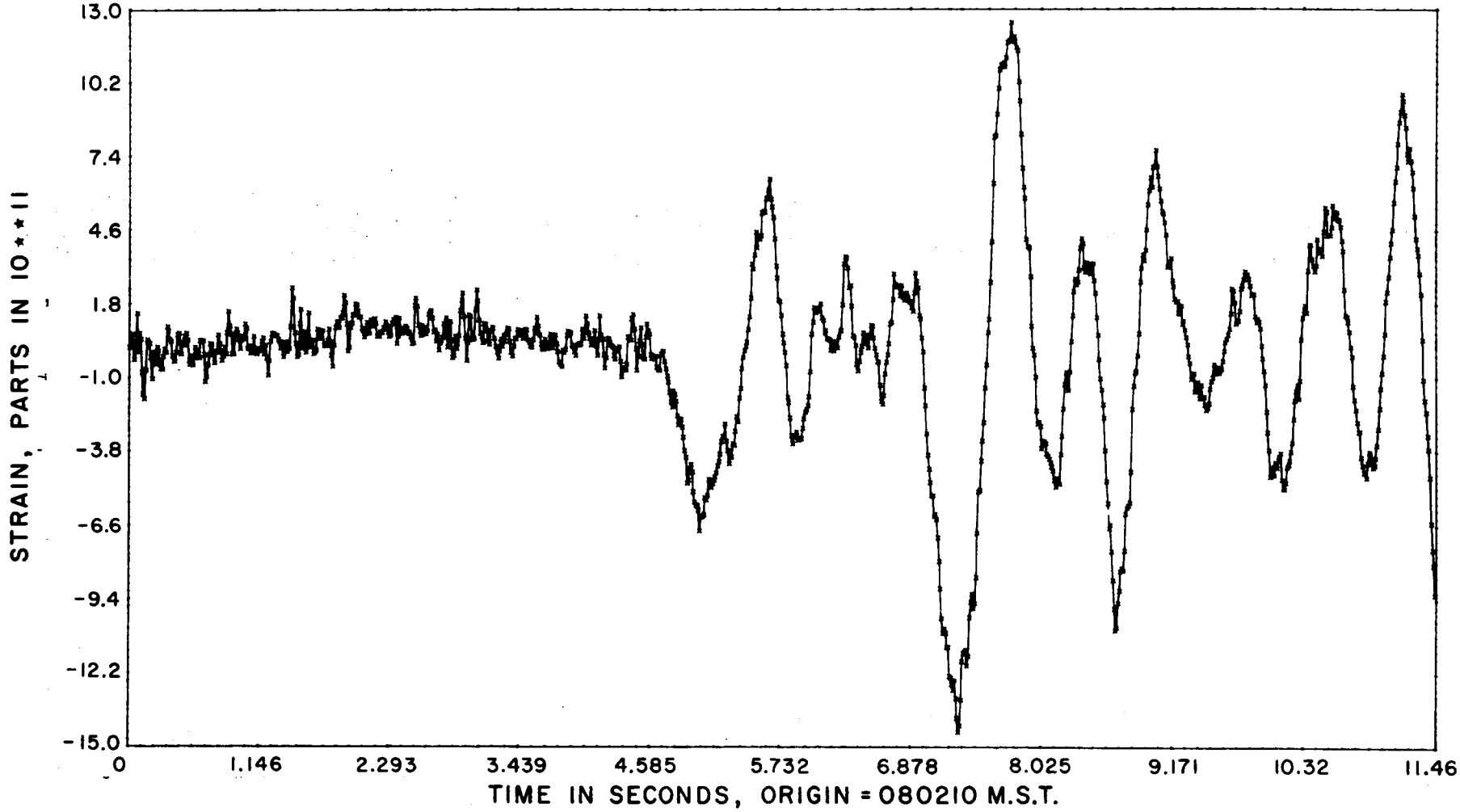

FIRST MOTION OF NUCLEAR EXPLOSION BOXCAR,
26 APRIL 68 START AT 080210 M.S.T.

Fig. 11